Available online at www.sciencedirect.com

SCIENCE DIRECT®

Catalysis Today 100 (2005) 145–150

CATALYSIS TODAY

www.elsevier.com/locate/cattod

Interpretation of kinetic data with selected characterizations of active sites

M. Schmal*, M.M.V.M. Souza, N.S. Resende, A.L. Guimarães,
C.A. Perez, J.G. Eon, D.A.G. Aranda, L.C. Dieguez

NUCAT/PEQ/COPPE—Federal University of Rio de Janeiro, C.P. 68502, 21945-970 Rio de Janeiro, Brazil

Abstract

Interpretation of kinetics is the focus of this contribution based on our experiences and particularly with selected characterizations besides the commonly reaction kinetic data in a differential reactor. The usual reaction kinetic models, such as Langmuir–Hinshelwood (L-H) and power law equations were used for three different cases besides one or two spectroscopic surface characterizations, allowing explaining the kinetic parameters.

The activity and selectivity are dependent on the catalyst and if they are structure sensitive, they depend strongly on the surface active sites, suffering transformations during the reaction, which have to be taken in account. FTIR and ISS measurements in situ explain the interface metal oxide site formation during CO oxidation and methane reforming and XPS data the structure transformation at the surface after different pre-treatment and propane oxidation. It was observed that in reducible oxide supports the oxygen is responsible for the surface interaction between different structures, affecting strongly the reaction rate.

Keywords: Kinetics; Characterizations in situ; Oxidation of methane and propane; Reforming of methane; Reducible oxide

1. Introduction

Catalysis and kinetics are still very important in homogeneous and heterogeneous reactions for industrial applications. Although most industrial processes were resolved during the past century, there are space for new developments of catalysts and processes in environment, fuel cells, natural gas conversion, new materials and nowadays in biotechnology. The main questions arising from industrial point of view are the stability and selectivity. From the scientific point of view it urges to questions concerning the understanding of the reaction mechanism and the kinetics.

Catalysts break forces, which inhibit the reaction of molecules and provide increasing reaction rates, involving adsorption–desorption. If the reaction is structure sensitive, the activity and selectivity are dependent of the particle sizes or surface-active sizes. Therefore, the reaction kinetics, usually described by the well-known Langmuir–Hinshelwood (L-H) models, must take in account the transient behavior of the surface during the reaction itself, modifying the sites and the adsorption–desorption phenomena and consequently the reaction mechanism. Therefore, the true kinetic is obtainable after surface characterization with reactions.

However, characterization techniques are in general very complex and nowadays they are so broad and overestimated that would not help understanding the surface kinetics. Most of the characterizations could be limited into two or three spectroscopic techniques, besides the conventional kinetic experiments and thermochemical experiments by varying the different parameters and labeled molecules.

The objective of this review is to present recent developments in our experience and to explain why kinetics must be studied through surface reactions using spectroscopic techniques for the determination of surface active sites using model reactants and selected reactions. From the

---

* Corresponding author. Fax: +55 21 2562 8300.
E-mail address: schmal@peq.coppe.ufrj.br (M. Schmal).

0920-5861/$ – see front matter © 2004 Elsevier B.V. All rights reserved.
doi:10.1016/j.cattod.2004.12.014

understanding of active surface sites the reaction mechanism could be explored and the reaction kinetic is explained. In the following sections we present three examples.

2. FTIR "in situ" of low-temperature CO oxidation over Pt/TiO_2 catalyst

Low temperature oxidation of carbon monoxide is an important reaction in environmental catalysis, the challenge being to lower significantly the light off temperature of the catalysts. Many research groups have been looking for new catalysts or investigating the mechanism of the reaction. In the last 20 years, fundamental studies have focused on platinum foils and single crystals, as well as supported platinum catalysts [1–4].

Graham and Linch [4,5] described transition effects between low and high conversions for specific reaction conditions; they used a general Langmuir–Hinshelwood model for CO islands at the surface undergoing oxidation–reduction phenomena. However, the classical L-H kinetic model based on weak adsorption of molecular oxygen competing with strong adsorption of carbon monoxide, described by Engel and Ertl [6], is still widely used. Several studies in the CO oxidation with different catalysts were reported in the literature [1–25].

Here we selected a Pt/TiO_2 catalyst and followed the kinetic performance in the CO oxidation. The kinetic results complemented by FTIR data in situ would explain the redox mechanism, allowing interpreting the effect of the support on the rate of CO_2 production by light off tests.

The platinum catalyst was prepared by impregnated on bulk titania, by using hexachloroplatinum acid solution and then dried at 393 K and calcined under air flow at 773 K for 4 h as described elsewhere [25]. The nominal concentration of platinum was 1 wt%.

The catalytic experiments were performed in a micro-reactor at atmospheric pressure at a temperature range of 373–673 K. The catalyst (ca. 250 mg) was pre-treated in helium (150 ml/min) at 823 K for 1 h and subsequently reduced at 773 K (10 K/min) with flowing 2% H_2/Ar (50 ml/min) for 2 h. The reaction mixture consisted of 4.7% CO/He and 5.2% O_2/He, balanced with He flow (150 ml/min; space velocity = 25,000 h^{-1}) [25].

The Arrhenius plot showed that the apparent activation energy was 57 kJ/mol, being in good agreement with that reported in the literature for Pt/γ-Al_2O_3 catalysts [1,19]. For temperatures bellow 600 K it has been suggested that CO and O_2 adsorptions are rate-determining steps for the CO oxidation reaction, because Pt is highly and homogeneously dispersed on TiO_2 with the formation of a great amount of active sites [25].

FTIR observations were performed aiming to determine the surface state of platinum (Pt^0 or Pt^{2+}) after coadsorption of CO and O_2 with increasing temperature of desorption. The catalyst was placed on a self-supported sample (thin disk wafer of 18 mm diameter and 25 mg). The disk was placed in a sample holder and introduced into a cell, which allowed in situ reduction and reaction. Two kinds of pre-treatments were done for comparison. In the first case all samples were reduced at 573 K with flowing H_2 (50 ml/min) for 1 h and evacuated for 1 h at the same temperature prior cooling to room temperature, followed by an uptake of a mixture of CO and O_2 (1:1) at 20 Torr and 303 K for 30 min. The infrared spectra were recorded on a Fourier transform infrared spectrometer (Perkin Elmer system-2000), after evacuation for 1 h at the same temperature. The sample was heated up at 10 K/min and spectra were taken at every 100 K. In a second mode of pre-treatment, the sample was calcined and treated under vacuum at 573 K, followed by adsorption of a mixture of CO and O_2 (1:1) at 573 K.

Fig. 1 shows the FTIR spectra obtained for the catalyst. The intense band around 2070 cm^{-1} is attributed to CO linearly adsorbed on Pt^0 just after reduction [25]. With increasing temperature, a slight shift of this band towards lower frequencies was noted and a second band emerged at 2120 cm^{-1}, corresponding to CO adsorbed on platinum oxide [8,15]. The band attributed to CO linearly adsorbed on Pt^0 disappeared at 573 K, remaining only the band of CO adsorbed on Pt oxide. These results are in good agreement with the literature [10]. Although some authors observed bridged CO after adsorption on reduced Pt, this species was not detected here. However, the band attributed to CO linearly adsorbed on Pt^0 disappears just at a lower temperature, around 473 K, suggesting that the presence of titanium oxide favored the oxidation of Pt^0.

FTIR results obtained on calcined samples after exposure to CO + O_2 mixture at 573 K for 30 min and after evacuation showed a sharp band indicating adsorption of CO on platinum oxide. This band appears at 2120 cm^{-1} but a slight shoulder was also observed at 2070 cm^{-1}, indicating adsorption of CO on Pt^0. This suggests some reduction of the PtO surface by CO, even at this temperature.

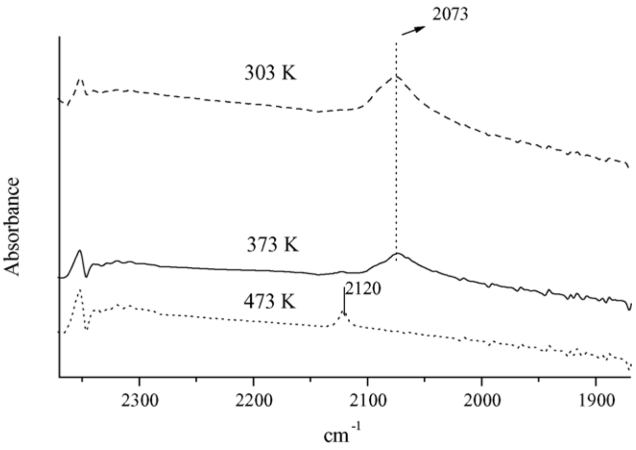

Fig. 1. FTIR after adsorption of a mixture of CO + O_2, and desorption from 303 to 473 K, (CO/O_2 = 1, P_{CO+O_2} = 22 Torr), on 1% Pt/TiO_2 reduced at 573 K.

This catalyst exhibited high activity and stability, which can be attributed not only to the high Pt dispersion but also to the transient surface modification. FTIR results show that CO is easily adsorbed on Pt sites and is then transferred to TiO_2, as already commented in the literature [19], which suggests the participation of titania in the reactivity of platinum. In addition TiO_x species are formed due to the SMSI effect [12], which probably facilitates the CO transfer for reduction at the interface of the titanium species. Vacancies are formed due to the reduction of Ti^{4+} to Ti^{3+}, allowing the oxygen transfer and enhancing desorption.

Therefore, the introduction of oxygen into the vacancies of TiO_x and the spillover phenomena occurring during CO oxidation explain the mechanism of adsorption–desorption, described by the Langmuir–Hinshelwood and consequently the kinetic of this reaction, as discussed elsewhere [25].

3. ISS and FTIR "in situ" of methane reforming

The main objective of the second case is to explain the bifunctional mechanism in the kinetics proposed for the dry reforming of methane with a Pt/ZrO_2 catalyst, using ISS measurements "in situ". Despite the fact that CH_4–CO_2 reforming has been studied extensively [26–35], less emphasis has been given on fundamental understanding of the reaction kinetics. Wei and Iglesia [36] performed kinetic and isotopic measurements that led to a sequence of elementary steps for the methane reforming, using isotopic mixtures such as $CH_4/CD_4/CO_2$. The turnover rates allowed the direct comparison of reactivity of Ni and noble metal catalysts for the methane reforming.

Bradford and Vannice [30–32] proposed a complete and consistent reaction model for CH_4–CO_2 reforming, based on CH_4 activation to form CH_x and CH_xO decomposition as the rate-determining steps, fitting well the experimental data for Ni [30] and Pt catalysts [31]. Although they had considered the roles of three types of sites (metal, support and metal–support interface), their proposed kinetic model included only one type of active site. However, the kinetic results for this catalyst suggests a bifunctional mechanism, which can be verified by ISS and FTIR complementary experiments.

Experimental details concerning the material and characterizations are presented elsewhere [37]. The rate-determining steps in our model are the decomposition of CH_4 and the subsequent reaction of CH_x fragments with CO_2 adsorbed species. For catalysts that kinetically inhibit excessive carbon deposition, like zirconia-containing catalysts described here, the surface concentration of carbon at the metal surface (in the form of CH_x) is at steady state and remains constant, i.e., the rate of CH_x decomposition equals that for CH_x reaction with CO_2 adsorbed species. Assuming two independent balances of sites, the reaction rate of methane was derived and presented good correlation with the experimental results [38].

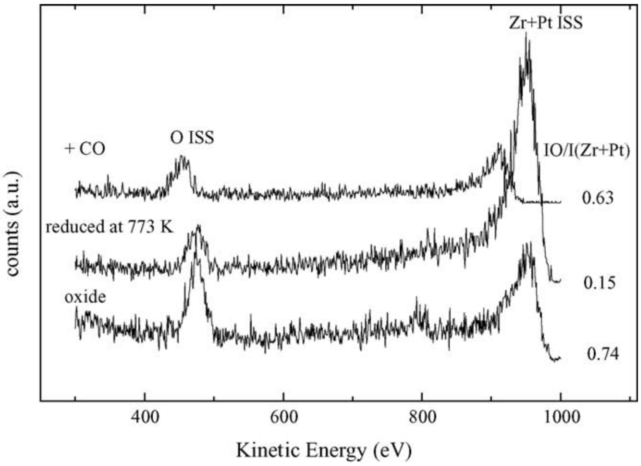

Fig. 2. ISS measurements on oxide and reduced Pt/ZrO_2 catalyst and after CO adsorption.

The surface state of Pt/ZrO_2 catalyst and its capacity to adsorb CO was studied by ISS in situ, which allows identifying the Zr atoms on the first atomic layer. The results are shown in Fig. 2. It is noteworthy that the peak ascribed to Pt and Zr atoms represents basically the Zr atoms, since the content of Pt was only 1 wt%. The enhancing intensity of the Zr + Pt peak after reduction at 773 K (the decrease in the IO/I(Zr + Pt) ratio shown in the figure) represents the increase in the surface zirconium atoms. After CO adsorption, Zr atoms also interact with CO, decreasing the Zr + Pt peak intensity and increasing the ratio IO/I(Zr + Pt).

The interaction of CO with Pt–ZrO_2 interface was also analyzed by FTIR spectroscopy. The IR spectra of CO desorption on Pt/ZrO_2 catalyst is displayed in Fig. 3. The spectra showed a small band at 2178 cm^{-1} at 298 K, which was attributed to the linear adsorbed CO species on cationic sites (either Zr^{4+} or Zr^{3+}). This adsorption involves the σ-donation type to coordenatively unsatured surface cationic sites (cus), acting as Lewis acid centers, according to previous works [38].

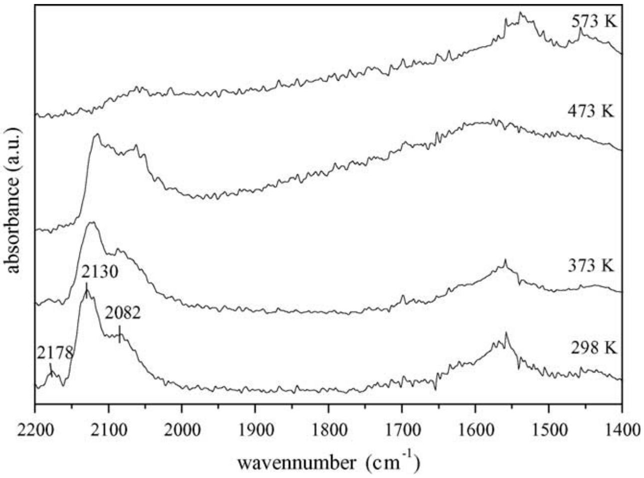

Fig. 3. FTIR spectra of CO for Pt/ZrO_2 reduced at 773 K after desorption at different temperatures.

The Pt/ZrO_2 catalyst reduced at 773 K showed also an intense band at 2130 cm^{-1}, which can be associated to CO adsorption on Pt–ZrO_2 interface, that means, on Pt sites interacting strongly with zirconia. The increase in the vibration frequency of CO can be explained by an electron transfer phenomenon from platinum particles to partially reduced zirconia, which decreases the Pt–CO bond strength. Dilara and Vohs [34] also observed the CO adsorption on the Pt–ZrO_2 interface and proposed a bonding configuration on that the carbon end of the CO molecule would be bounded to platinum while the oxygen end interacts with Zr^{n+} cations on the surface of the oxide.

In conclusion, the interface Pt–Zr^{n+} and the Pt sites were observed using in situ techniques and support the mechanistic dual site model proposed for the reaction rate kinetics [38].

4. XPS of propane combustion

This third case is to verify what modifications occurring at the surface of a Pd–Ce/Al_2O_3 catalyst during the oxidation of propane. This reaction was extensively studied in the literature [39–42], however the surface catalyst is liable to contamination, affecting the surface active sites and consequently the kinetics. The main reactions that may occur favoring the hydrogen production for fuel cells are:

$$C_3H_8 + 5O_2 \rightarrow 3CO_2 + 4H_2O$$

$$C_3H_8 + 3H_2O \rightarrow 3CO + 7H_2$$

$$C_3H_8 + 6H_2O \rightarrow 3CO_2 + 10H_2$$

Palladium active sites are influenced by several factors, such as the particle mean size, the support interaction and the nature of the precursor salts. The particle size plays an important role for structure-sensitive reactions since, either the site coordination, such as kink, step and terrace atoms, or the crystal orientation affect the catalytic reactivity. The metal–support interaction also contributes to change in Pd sites, especially when they are supported on reducible transition metal oxides.

Restructuring of catalytic sites at the interface, electronic transfer or encapsulation of metal particles by reduced support species are some of the explanations that are found in literature to define metal–support interaction nature [43].

Gama alumina (Harshaw) with a surface area of 208 m^2/g was used as support. Samples were prepared with 1% of palladium, using the impregnation method. The catalyst was prepared in two steps. First, impregnation of cerium oxide over the alumina support, using a cerium acetylacetonate solution with a concentration of 17% of cerium oxide, corresponding to a theoretical monolayer, calcined with flowing air at 773 K for 4 h, as described elsewhere [44]. The BET area was 193 m^2/g and pore volume 0.40 cm^3/g. This system was well characterized as reported previously [44,47]. Then, Pd was impregnated similarly with 1% metallic palladium. The Pd precursor was $Pd(acac)_2$ (Aldrich, 99%). Toluene (Vetec, 99%) was used to dissolve $Pd(acac)_2$ and wet impregnation was employed at room temperature for 24 h, followed by filtration. After impregnation the catalysts were dried in a muffle at 393 K for 18 h, followed by calcination in an aerated muffle furnace at 773 K for 4 h PdCe, as described elsewhere [45,46].

The catalytic reaction test was carried out in a microreactor, using 25 mg of the catalyst diluted in 250 mg of glass. Reaction was performed flowing a mixture of 150 ml/min of 1000 ppm C_3H_8/He and different O_2/C_3H_8 ratios (R) with balance He. The reaction temperature was 673 K. The reaction of propane oxidation was performed at an O_2/C_3H_8 ratio $R = 5$. The reaction was stable after 20 h of time on stream. In addition, water was introduced through a saturator under controlled temperature, such as the concentration of water was around 3%.

The reaction rate was determined using the general power rate law according to:

$$\text{Rate}_{C_3H_8} = k(C_{C_3H_8})^{\alpha}(C_{O_2})^{\beta}(C_{H_2O})^{\gamma}$$

where k is the reaction constant.

The reaction order of α and β are 0.3 and 0.6, respectively in the absence of water. On the other hand, with water the effect of the partial pressure of oxygen exhibited negative values of $\beta = -0.7$. We observed re-dispersion of Pd after introducing water in the reactants, which means that these reactants are strongly adsorbed provoking a negative order for $\gamma = -0.6$ [48].

X-ray photoelectron spectroscopy (XPS) was performed in a Perkin Elmer instrument using radiation source Al Kα, with energy of 1486.6 eV and 12 kV. The acquisition time was 0.2 s per sweep and scanning of 20, 100, 50, 30 and 10 sweeps for elements Ce 3d, Cl 2p, Al 2p, C 1s and O 1s, respectively. For palladium (Pd 3d), 30 and 200 sweeps were used in order to observe if photo-reduction of palladium might occur after exposure to the X-ray beams. The correction for charging effects was made with the C 1s peak at 284.6 eV. Analyses were performed recording spectra of Pd 3d, Ce 3d, Cl 2p, Al 2p, C 1s and O 1s, for the Pd/Al_2O_3 and Pd/CeO_2/Al_2O_3 systems. Samples were pre-treated with hydrogen and propane oxidation in the presence or absence of water under stoichiometric reaction condition in a pre-chamber. After evacuation and cool down, samples were introduced in the UHV chamber and spectra were obtained as described elsewhere [47]. Aiming to identify the oxidation state of palladium during the oxidation of propane, the samples were submitted separately to 1% C_3H_8/He with 5% O_2/He, and 1% C_3H_8/He, 5% O_2/He with 5% H_2O, under stoichiometric conditions ($R = 5.0$), at 150 ml/min and at 673 K for 60 min. These experiments were performed in a pre-chamber and then transferred to the UHV chamber.

The XPS results for Pd/CeO_2/Al_2O_3 after reduction also evidence the presence of metallic Pd (335.4 eV), similar to the reduced Pd/Al_2O_3. However, after oxidation and with water, the band shift of Pd was greater than 2.0 eV, which

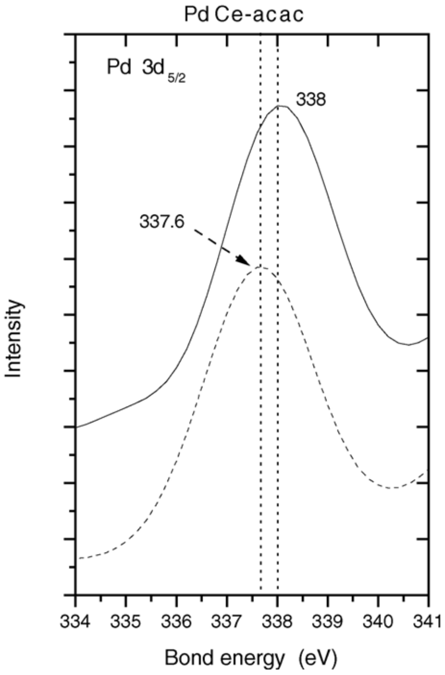

Fig. 4. XPS spectra after successive treatment cycles: (- - -) reduction + 3% H_2O/He at 673 K, (—) reduction + O_2/He at 673 K.

also corresponds to a higher oxidation state, probably PdO_2 (338 eV). The binding energy of $Pd_{5/2}$ for the PdCe-acac was 338.0 and 337.6 eV, without and with water, respectively (Fig. 4).

The O/Al ratio of the theoretical value of Al_2O_3 is $\geq$1.50. The O/Al ratio with the incorporation of CeO_2 increased drastically, ranging from 3.70 after reduction to 6.80 after oxidation and 7.20 with water (Table 1). This is approximately three times in relation to the precursors without CeO_2. In conclusion, this big increase of O/Al ratio and the shift of the binding energy of Pd $3d_{5/2}$ reveal the incorporation of oxygen, suggesting storage of oxygen in the CeO_2 lattice and in the palladium after the reaction cycle. In addition, the band shift of the binding energy of Pd towards 337.2 eV, which is attributed to a higher oxidation state of palladium, according to the literature [47]. This shift evidences that PdO and PdO/PdO_2 interfaces coexist, which are the active sites for the oxidation reaction [47].

In conclusion, XPS results display changes of the Pd and CeO_2 structure during the propane oxidation with or without water, which indeed, justifies the modification of the reaction order in the reaction rate.

Table 1
Bond energy for Pd $3d_{5/2}$ and atomic ratios by XPS for Pd/CeO_2/Al_2O_3

Sample	Treatment	Bond energy (eV)	Atomic ratio			
			Pd/Al	Cl/Al	O/Al	O/Ce
PdCe-acac	C_3H_8/O_2	338.0	0.11	0.03	6.80	3.60
	$C_3H_8/O_2/H_2O$	337.6	0.12	0.03	7.20	3.80

^{1}Pd $3d_{5/2}$ ^{2}Al 2p ^{3}Cl 2p ^{4}O 1s ^{5}Ce 3d total.

5. Concluding remarks

The reaction rates or turnover number were obtained from experimental results for different structure sensitive reactions and catalysts, which are strongly dependent on the surface active sites. The surface sites are suffering transformations during the reaction, which have been taken in account by using different spectroscopic measurements.

Characterizations in situ for the Pt/TiO_2 catalyst explain the great amount of vacancies formed due to the reduction of Ti^{4+} to Ti^{3+}, allowing the oxygen transfer during the CO oxidation.

ISS and FTIR results showed interfacial Pt–Zr^{n+} and Pt sites for the Pt/Zr/Al_2O_3 catalysts, which explain the mechanistic dual site model proposed for the reaction rate kinetics of methane reforming.

Finally, XPS results display changes of the Pd and CeO_2 structure for the Pd/Ce/Al_2O_3 catalysts during the propane oxidation with or without water, justifying the modification of the reaction order in the reaction rate.

Noteworthy is that in all reducible oxide supports the oxygen is responsible for the surface interaction between different structures and the interaction with the reacting molecules, affecting strongly the rate of reaction and the kinetic parameters, in particular the adsorption–desorption constants.

References

[1] Y. Cai, H.G. Stenger Jr., C.E. Lyman, J. Catal. 161 (1996) 123.
[2] P. Thormählen, M. Skoglundh, E. Fridell, B. Anderson, J. Catal. 188 (1999) 300.
[3] A. Bourane, D. Bianchi, J. Catal. 202 (2001) 34.
[4] W.C. Graham, D. Linch, AIChE J. 36 (1990) 1796.
[5] W.C. Graham, D. Linch, AIChE J. 33 (1987) 792.
[6] T. Engel, G. Ertl, Adv. Catal. 28 (1) (1979).
[7] B.N. Racine, R.K. Herz, J. Catal. 137 (1992) 158.
[8] M. Primet, J.M. Basset, M.V. Mathieu, M. Prettre, J. Catal. 29 (1973) 213.
[9] M. Primet, J. Catal. 88 (1984) 273.
[10] J.A. Anderson, J. Chem. Soc. Faraday Trans. 88 (8) (1992) 1197.
[11] G.J. Arteaga, J.A. Anderson, C.H. Rochester, J. Catal. 184 (1999) 268.
[12] J.A. Anderson, Catal. Lett. 13 (1992) 363.
[13] N.S. Resende, J.-G. Eon, M. Schmal, J. Catal. 183 (1999) 6.
[14] J.L. Margitfalvi, I. Borbáth, M. Hegedús, E. Tfirst, S. Góbölös, K. Lázár, J. Catal. 196 (2000) 200.
[15] C.C. Chang, L.L. Hegedus, J. Catal. 57 (1979) 361.
[16] N.W. Cant, J. Catal. 62 (1980) 173.
[17] R.K. Herz, S.P. Marin, J. Catal. 65 (1980) 281.
[18] R. Barth, R. Pitchai, R.L. Anderson, X.E. Verykios, J. Catal. 116 (1989) 61.
[19] G.B. Fisher, S.H. OH, J.E. Carpenter, C.L. Dimaggio, S.J. Schmieg, in: A. Crucq, A. Frennet (Eds.), Catalysis and Automotive Pollution Control, Elsevier, Amsterdam, 1987.
[20] B.E. Hayden, K. Kretzschmar, A. Bradshaw, R.G. Greenler, Surf. Sci. 149 (1985) 394.
[21] R.A. van Santen, J.W. Niemantsverdriet, Handbook-Chemical Kinetics and Catalysis, third ed. Eindhoven University of Technology, 1994.

[22] H. Liu, A.I. Koslov, A.P. Koslov, T. Shido, K. Asakura, Y. Iwasawa, J. Catal. 185 (1999) 252.

[23] M. Vaarkamp, J.T. Miller, F.S. Modica, D.C. Koningsberger, J. Catal. 163 (1996) 294.

[24] M. Manzoli, Appl. Catal., B: Environ. 52 (2004) 259.

[25] N.S. Resende, J.G. Eon, M. Schmal, Appl. Catal., B, submitted for publication.

[26] J.H. Bitter, K. Seshan, J.A. Lercher, J. Catal. 171 (1997) 279.

[27] A.N.J. Van Keulen, K. Seshan, J.H.B.J. Hoebink, J.R.H. Ross, J. Catal. 166 (1997) 306.

[28] S.M. Stagg, E. Romeo, C. Padro, D.E. Resasco, J. Catal. 178 (1998) 137.

[29] S.M. Stagg-Williams, R. Soares, E. Romero, W.E. Alvarez, D.E. Resasco, Stud. Surf. Sci. Catal. 130 (2000) 3663.

[30] M.C.J. Bradford, M.A. Vannice, Appl. Catal., A: General 142 (1996) 97.

[31] M.C.J. Bradford, M.A. Vannice, J. Catal. 173 (1998) 157.

[32] M.C.J. Bradford, M.A. Vannice, Cat. Rev.-Sci. Eng. 41 (1) (1999) 1.

[33] A.M. O'Connor, Carbon dioxide reforming of methane over Pt/ZrO_2 catalysts, Ph.D. thesis, University of Limerick, Irlanda, 1998.

[34] P.A. Dilara, J.M. Vohs, J. Phys. Chem. 99 (47) (1995) 17259.

[35] S. Roberts, R.J. Gorte, J. Phys. Chem. 95 (14) (1991) 5600.

[36] J.M. Wei, E. Iglesia, J. Catal. 224 (2) (2004) 370.

[37] M.M.V.M. Souza, D.A.G. Aranda, M. Schmal, J. Catal. 204 (2001) 498.

[38] M.M.V.M. Souza, D.A.G. Aranda, C.A.C. Perez, M. Schmal, Phys. Status Solidi A 187 (2001) 297.

[39] F.H. Ribeiro, M. Chow, R.A. Dalla Betta, J. Catal. 146 (1994) 537.

[40] P. Marécot, A. Fakche, B. Kellali, G. Mabilon, M. Prigent, J. Barbier, Appl. Catal., B: Environ. 3 (1994) 283.

[41] S. Salasc, V. Perrichon, M. Primet, M. Chevrier, F. Mathis, N. Moral, Catal. Today 50 (1999) 227.

[42] R. Burch, E. Halpin, M. Hayes, K. Ruth, J.A. Sullivan, Appl. Catal., B: Environ. 19 (1998) 199.

[43] S. Bernal, G. Blanco, M.A. Cauqui, M.P. Corchado, C. Larese, J.M. Pintado, J.M. Rodriguez-Izquierdo, Catal. Today 53 (1999) 607.

[44] R.S. Monteiro, L.C. Dieguez, M. Schmal, Catal. Today 65 (2001) 77.

[45] M. Schmal, D.A.G. Aranda, F.B. Noronha, A.L. Guimarães, R.S. Monteiro, Catal. Lett. 64 (2000) 163.

[46] A.B. Gaspar, L.C. Dieguez, Appl. Catal., A 201 (2000) 241.

[47] A.L. Guimarães, L.C. Dieguez e, M. Schmal, J. Phys. Chem. B 107 (2003) 4311.

[48] A.L. Guimarães, L.C. Dieguez e, M. Schmal, An. Acad. Bras. Cienc. 76 (2004) 825.